

# **NO<sub>x</sub> emissions and turbulent flow field in a partially premixed bluff body burner with CH<sub>4</sub> and H<sub>2</sub> fuels**

**Marcin Dutka<sup>1,\*</sup>, Mario Ditaranto<sup>2</sup>, Terese Løvås<sup>1</sup>**

<sup>1</sup> Department of Energy and Process Engineering, Norwegian University of Science and Technology, Kolbjørn Hejes vei 1b, 7491 Trondheim, Norway

<sup>2</sup> SINTEF Energy Research, Sem Sælands vei 11, 7034 Trondheim, Norway

\* corresponding author e-mail: marcin.d.dutka@gmail.com

## **Abstract**

The increased need for fuel flexibility and CO<sub>2</sub> capture solutions (CCS) in the power and industrial sectors has led to higher focus on hydrogen containing fuels. The high reactivity and combustion temperature in hydrogen flames are a source of high nitrogen oxides (NO<sub>x</sub>) and a barrier to the implementation of traditional dry lean premixed low NO<sub>x</sub> burner technology. The present experimental study investigates emissions of NO<sub>x</sub> and characterises the turbulent flow field above a promising burner concept based on partially premixed bluff body (PPBB) strategy. The PPBB burner configuration allows for a rapid mixing of fuel and air through multiple fuel injection in the accelerating air stream, followed by a flame stabilization process controlled by a bluff body. The measurements were conducted using methane, hydrogen, and a methane-hydrogen mixture 50/50 mass fraction as fuels and at various burner thermal loads ranging from 10 kW to 25 kW. The turbulent flow field characterisation was made by Particle Image Velocimetry (PIV) without the combustion chamber and in selected operation modes. Several burner parameters were varied, as the position of the bluff body and the fuel distribution. Shifting the burner lance controlling the bluff body position to accelerate the air flow resulted in lower NO<sub>x</sub> emissions, although negatively affecting the flame stability and generating incomplete combustion. Supplying fuel through secondary fuel ports had opposite effect on NO<sub>x</sub> emissions depending on the fuel: an increase for methane and a decrease for hydrogen.

The temperature of the chamber has significant impact on NO<sub>x</sub> emissions and was quantified in the study with a 50 % increase from a chamber temperature of 700 °C to 1050 °C. NO<sub>x</sub> emissions are generally higher as the hydrogen content in the fuel increases. The lowest achieved NO<sub>x</sub> emissions are 26 and 66 ppm at 3% O<sub>2</sub> dry for methane and hydrogen respectively.

## 1. Introduction

Industrial boilers and furnaces fired by fossil fuels are a major source of carbon dioxide ( $\text{CO}_2$ ) emissions to the atmosphere [1]. A scenario that allows for a reduction of global  $\text{CO}_2$  emissions from fossil fuel based processes is utilization of Carbon Capture and Storage (CCS) technologies. Boilers and furnaces are often large-scale combustion facilities and pre-combustion  $\text{CO}_2$  capture technology is considered as suitable for such applications [2]. The concept of pre-combustion capture is based on converting the chemical energy of the hydrocarbon fossil fuel into hydrogen ( $\text{H}_2$ ) by reforming or gasification, and separation of the  $\text{CO}_2$  formed in that process.  $\text{H}_2$  can then be used as fuel in industrial burners without  $\text{CO}_2$  emissions, with the additional advantage of avoiding other pollutants such as carbon monoxide, unburned hydrocarbons, and particularly particles. Most studies indicate that burners designed for natural gas experience significant problems such as mechanical and thermal damages due to the change in flame speed when firing high  $\text{H}_2$  containing fuels. Therefore, there is considerable effort to develop burners that are fuel flexible with regard to the fuel  $\text{H}_2$  content while keeping low emissions characteristics. Such burners could be used not only in new devices, but also as a retrofit in a large number of existing installations at low cost.

Many combustion studies have been conducted using  $\text{H}_2$  enriched methane ( $\text{CH}_4$ ) or natural gas [3-11], amongst others. These studies revealed that addition of  $\text{H}_2$  to conventional fuel results in significant extension of the lean stability limit of the burner operation range [3-7]. However, high  $\text{H}_2$ -air flame speed increases the risk of flashback in premixed systems and results in changes of the flame shape [4,5]. This challenge is so serious that to date the low  $\text{NO}_x$  dry lean premixed technology has not been successfully adapted to fuels containing high concentrations of  $\text{H}_2$ . To circumvent that issue, concepts have even been proposed based on recirculating exhaust gases and operate the burner in oxygen-depleted atmosphere instead [12,13]. Furthermore, the different thermodynamic properties of  $\text{H}_2$  affect the flow field above the burner in many ways (calorific value, density, differential diffusion) requiring flow field

analysis to ensure that the burner can operate with H<sub>2</sub> and maintain high combustion efficiency and low pollutant emissions [8-10].

Adiabatic flame temperature of H<sub>2</sub>-air flames is higher than that of methane-air flames. This parameter has a significant impact on harmful emissions of nitrogen oxides (NO<sub>x</sub>), because most NO<sub>x</sub> generated in industrial combustion systems come from highly temperature-dependent NO<sub>x</sub> formation mechanisms. Several NO<sub>x</sub> formation mechanisms contribute to total NO<sub>x</sub> emissions from combustion of gaseous fuels including the thermal (a.k.a. Zeldovich) route [14,15], the prompt (Fenimore) route [16], the nitrous oxide (N<sub>2</sub>O) intermediate route [17] and the NNH route [18]. Importance of these mechanisms depends on local temperature, local stoichiometric conditions and fuel composition. For example, prompt NO<sub>x</sub> is produced in hydrocarbon flames, but not in pure H<sub>2</sub> flames, because the prompt route requires carbon-containing radicals. In turn, significant amount of NO<sub>x</sub> can be formed via the N<sub>2</sub>O and NNH mechanisms in H<sub>2</sub> flames [19]. Therefore, depending on whether hydrocarbon fuel or H<sub>2</sub> is combusted, importance of various NO<sub>x</sub> formation routes may change. Another important factor is that NO<sub>x</sub> emissions are also affected by furnace temperature through the interaction of radiative heat transfer [20], therefore burner emission performance depends not only on the burner design itself, but also on the conditions in which it operates.

Generally, the higher H<sub>2</sub> concentration in the fuel, the higher the NO<sub>x</sub> emissions via the thermal route as seen in most practical flame studies [4,21-25]. However, increased temperature enhances all NO<sub>x</sub> kinetic routes described above and the intermediate radical concentrations such as OH, O, H, and CH play a very important role in the prompt NO reaction mechanism active for the hydrocarbon fuels in the mixture. All effects combined leads to a known behavior where the maximum NO<sub>x</sub> emissions when going from pure CH<sub>4</sub> to H<sub>2</sub> does not necessarily occur with pure H<sub>2</sub>. Studies that investigated H<sub>2</sub> addition throughout the whole range generally observe that the maximum is around 80 % volume H<sub>2</sub> [4]. In addition, fluid dynamic effects like fuel-air mixing and turbulence induced by each particular burner design also affect the

kinetics strongly. As a result, when Cozzi and Coghe [4] observes a roughly doubling in NO<sub>x</sub> emissions by going from pure CH<sub>4</sub> to pure H<sub>2</sub> in a non-premixed swirl stabilized burner, the radiant burner of Waibel et al. [26] showed emissions in the same range, and the flameless burner of Ayoub et al. [27] even experienced a decrease. Newbold et al. [28] measured NO<sub>x</sub> emissions from different types of burners but with identical conditions at the burner's exit and found that NO<sub>x</sub> emissions are reduced in bluff body stabilized flames relative to turbulent jet flames and also these flames are significantly shortened. Dally et al. [29] found that in turbulent non-premixed flames stabilized on a bluff body NO is generated either in the recirculation zone, which length is approximately that of the bluff body diameter, or further downstream of the neck zone. When the jet velocity increases and approaches blow off, the residence time decreases and NO decreases right across the flame [29]. With this knowledge, one may find a useful application of bluff bodies to stabilize the flame in a wide range of operating conditions and simultaneously achieve low NO<sub>x</sub> emissions.

The present study focuses on a novel burner concept [30,31] that produces partially premixed flames stabilized on a conical bluff body, hence referred to as the partially premixed bluff body (PPBB) burner. The characteristic feature distinguishing the PPBB burner from other types of bluff body burners is the fact that the diameter of the bluff body is greater than the diameter of the outer tube at the burner throat, representing a blockage ratio greater than 100%. Another difference is that most bluff body burners have a central fuel injection (e.g. [29,32-34]). Furthermore, the unique design of the PPBB burner is to make advantage of premixing fuel and air, beneficial for minimizing NO<sub>x</sub> production as discussed above, while avoiding flashback issues in the burner. Thanks to the burner head arrangement described in the experimental section, the burner allows rapid premixing of fuel and air shortly before combustion is stabilized by the bluff body. Staging of the fuel is possible and generates a partially premixed gas mixture. Because of these features, the PPBB burner is an appropriate candidate to operate as a multi-fuel burner suitable for combustion of CH<sub>4</sub>, H<sub>2</sub>, and mixtures of both.

Initial characteristics of NO<sub>x</sub> emissions of the burner have previously been investigated by the authors for CH<sub>4</sub> and H<sub>2</sub>-enriched CH<sub>4</sub> fuel mixtures and found that the PPBB burner has the potential to achieve low NO<sub>x</sub> emissions compared with commercially available solutions [35,36]. These studies used Central Composite Design methodology to assess various burner physical and operational parameters and showed that of all factors, H<sub>2</sub> content in the fuel has negative impact on NO<sub>x</sub> emissions [35]. 20 ppm NO<sub>x</sub> range was achieved with H<sub>2</sub>/CH<sub>4</sub> mixtures with H<sub>2</sub> mass fraction of 5 % to 30% (respectively 30 % and 70 % volume fraction) [36]. However, in these studies, pure H<sub>2</sub> was not included and the burner was tested in a chamber at a temperature reaching 390 - 400°C, which can be considered as a low temperature environment compared to most industrial furnaces. Another study from the authors [37] on the PPB burner focused exclusively on the non-reacting flow field behavior and showed that in the turbulent regime both the length of the recirculation zone and the recirculated flow fraction are rather independent of Reynolds number in which operate the PPBB burner under combustion mode.

In the present study, results from pure CH<sub>4</sub>, pure H<sub>2</sub> and 50 % mass fraction (i.e. 89 % H<sub>2</sub> volume fraction) mixture fuels are presented. The influence of the burner design parameters on NO<sub>x</sub> emissions is analyzed over a wide range of operating conditions for the particular bluff body design, including varying chamber temperature. The main goals of the paper are first to quantitatively investigate NO<sub>x</sub> emissions from the burner fueled by H<sub>2</sub> or CH<sub>4</sub> at various burner operation settings offering wide fuel flexibility capacity; secondly, to investigate the velocity flow fields behind the burner for non-reacting and reacting flows at identical flow conditions. The data obtained in the experiments are used to explain how various factors affect NO<sub>x</sub> emissions and the flow field in the unique burner design. With this knowledge, it is possible to correlate NO<sub>x</sub> emissions with the characteristic features of both non-reacting and reacting flow fields and assess the influence of the presence of the flame on the flow field in the cases of H<sub>2</sub>

and CH<sub>4</sub> combustion. The overall purpose is to identify the flow conditions that are favorable to minimization of NO<sub>x</sub> emissions in a practical burner.

## **2. Experimental approach and setup**

The burner – combustion chamber set up used in the experimental campaign is presented in Fig. 1 with a close up on the PPBB burner geometrical details. The PPBB burner consists of the central fuel lance terminated by a diverging conical burner head forming the bluff body and the outer tube. The outer tube ends with a converging section accelerating the air flow as it approaches the burner exit plan. The axial location referred to as the burner throat throughout this study is shown in Fig. 1. The fuel - air mixture leaving the outer tube passes the lance and creates a recirculation zone above the bluff body and a shear layer, where the flame is stabilized. Fuel provided to the burner can be distributed at the primary and secondary fuel ports and the velocity of the mixture at the burner throat can be controlled by shifting the lance axially relative to the outer tube. Flow rates of fuel and air to the burner were controlled with mass flow controllers. Primary and secondary fuel are controlled separately.

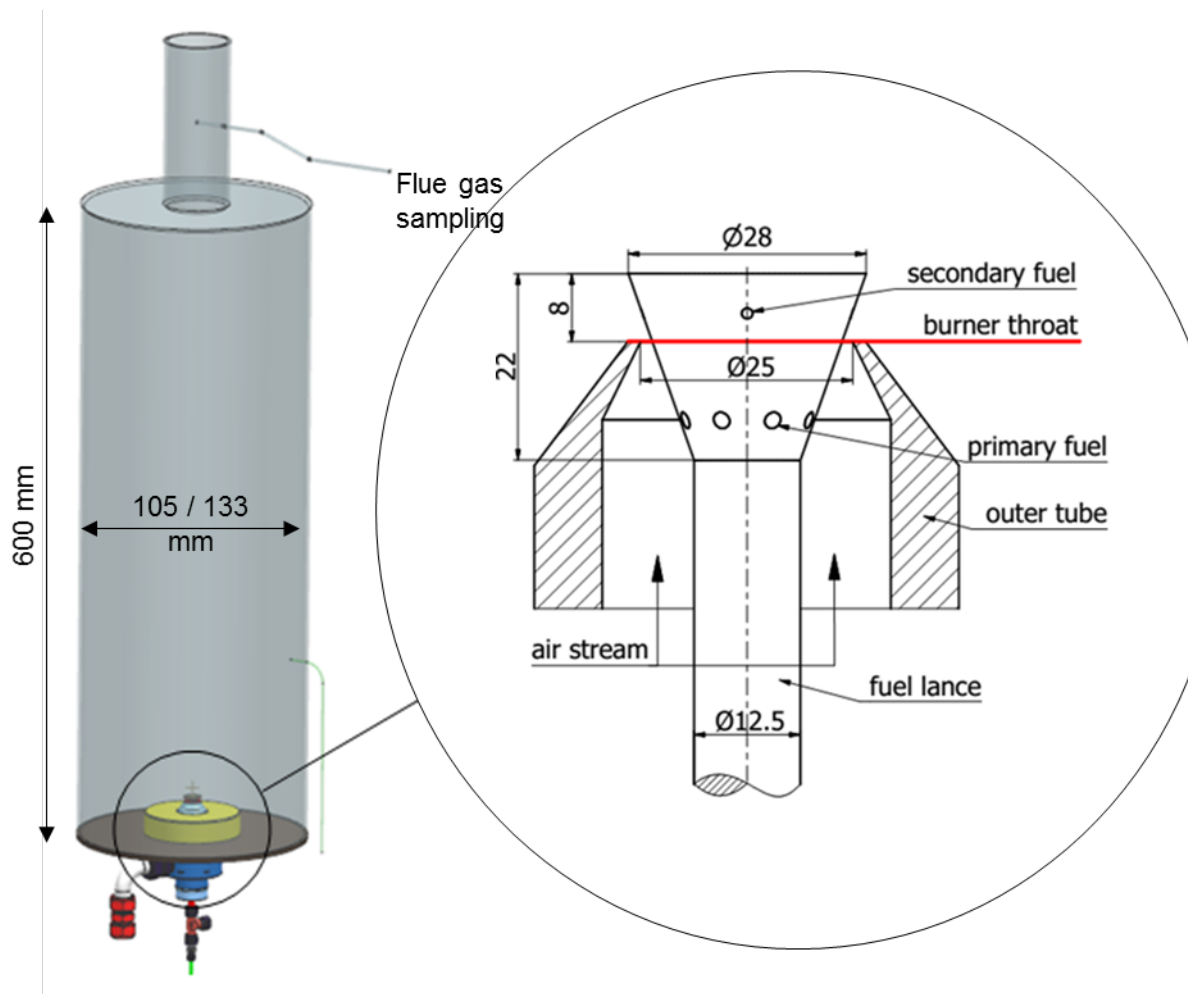


Fig 1— Burner – chamber setup and details of the PPBB burner geometry.

The PPBB burner was mounted at the base of a vertical cylindrical combustion chamber fitted with a convergent flow restriction at its end. Two chambers were used in order to investigate  $\text{NO}_x$  emissions from the burner and the effect of chamber wall temperature on  $\text{NO}_x$  emissions. Two combustion chambers, both 600 mm long, were used to investigate the effect of confinement ratio and wall temperature on the  $\text{NO}_x$  performance. One combustion chamber is made of stainless steel cylinder insulated with a 30 mm thick concrete layer in the inner side forming a 105 mm inner diameter. A copper coil located inside the insulation layer was used to water cool the chamber on its outer surface, as due to the low thermal conductivity and relatively high thickness of the concrete wall, it did not affect the inner chamber wall temperature. The second combustion chamber had an inner diameter of 133 mm, also made of stainless steel, but

insulated on the outer side using high temperature fiber insulation. The only role of the insulation was to ensure high temperature of the chamber wall in order to investigate NO<sub>x</sub> emissions for a wide range of the chamber temperatures.

Flue gases were sampled at the outlet of the chamber through a 5 points probe placed in the restricted section of the chamber. Gas sample was sucked through a gas analyzer (Horiba PG-250) for measuring NO<sub>x</sub>, O<sub>2</sub>, CO and CO<sub>2</sub>. NO<sub>x</sub> concentrations were measured with an accuracy of 1 ppm according to the instrument supplier. For NO<sub>x</sub> emissions measurement campaigns the burner was fueled with H<sub>2</sub>, CH<sub>4</sub>, and mixtures of those with an excess air of 15%. The burner thermal load was varied between 10 and 25 kW (based on lower heating value) at 5 kW increment. Several burner parameters were varied for each fuel and thermal load as shown in Table 1. The comparison of emission data between fuels can be misleading when expressed as dry volume fractions since the only product of combustion for H<sub>2</sub> is steam, therefore all NO<sub>x</sub> emissions results are converted and expressed in the unit of mg/kWh using thus the fuel LHV and mass flow rate as reference.

Table 1— Parameters used in the experimental studies.

Parameter	Value
Fuel	H <sub>2</sub> ; CH <sub>4</sub> ; H <sub>2</sub> /CH <sub>4</sub> (50/50 mass fraction)
Air/fuel equivalence ratio	1.15
Thermal load (kW)	10; 15; 20; 25
Lance position* (mm)	8; 12; 16
Secondary fuel fraction (% mass)	0; 10; 20; 30

\* *measured from the burner throat*

The NO<sub>x</sub> emissions parametric study based on Table 1 identified the burner settings with lowest NO<sub>x</sub> emissions for the different fuel mixtures. These settings were used in the part of the study focusing on the effect of chamber temperature on NO<sub>x</sub> emissions. Since the combustion chamber temperature cannot be controlled independently of burner thermal load the temperature of the chamber was monitored using three thermocouples. These thermocouples were mounted on the outer surface of the chamber wall, not exposed to the flame. When the

temperature was increasing,  $\text{NO}_x$  emissions were measured and recorded along with the maximum temperature reading of the chamber. Maximum temperature increase rate in the experiment was below  $1\text{ }^\circ\text{C/s}$ , while time interval for gas sample analysis was 10 seconds. It was found that the delay caused by the gas analyzer does not significantly affect the results and the  $\text{NO}_x$  emissions dependence on chamber temperature could be studied in this manner.

PIV measurements were performed at selected operating conditions as shown in Table 2 at a constant power load of 10 kW, in order to analyze the  $\text{NO}_x$  emission performance of the burner in relation to the near-burner aerodynamics. These measurements were limited to the near field above the bluff body and they were conducted without the combustion chamber.

Table 2 — Burner operating conditions used for PIV measurements. LP: lance position; SF: secondary fuel fraction; NR/R: Non-reacting/Reacting; LPX/Y: lance position at X mm from the burner throat, with air velocity adjusted to match that of lance position Y mm.

Case name	LP [mm]	SF [%]	$\text{CH}_4$	$\text{H}_2$ [NI/min]	Air	NR/R [-]
CH4LP8SF0	8	0	16.7	0	185.0	NR
CH4LP8/12SF0	8	0	16.7	0	86.9	NR
CH4LP8SF30	8	30	16.7	0	185.0	NR
CH4LP16SF0	16	0	16.7	0	185.0	NR, R
CH4LP16SF30	16	30	16.7	0	185.0	NR, R
H2LP8SF0	8	0	0.0	55.6	153.8	NR, R
H2LP8/12SF0	8	0	0.0	55.6	52.25	NR
H2LP8SF30	8	30	0.0	55.6	153.8	NR, R

The PIV setup used in the experimental campaign is presented in Fig. 2, consisting of a high repetition rate laser and a high-speed camera to measure the velocity flow field. The laser and the camera were synchronized by the LaVision DaVIS 8.2.1 software. Olive oil droplets and titanium dioxide ( $\text{TiO}_2$ ) particles were used as tracers in non-reacting and reacting cases, respectively and were seeded to the combustion air stream. A high-speed Nd: YLF, water-cooled, diode pumped, double cavity laser was used to form a laser sheet of approximately 0.5 mm thickness crossing the axis of the burner and illuminating the tracer particles in the measurement plane above the burner surface, as shown in Fig. 3.

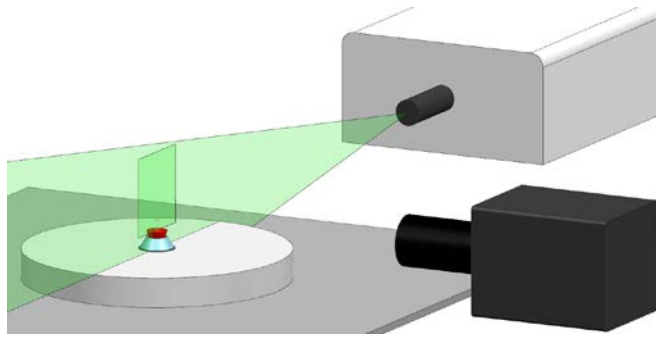


Fig. 2 — PIV set-up (camera's field of view marked with dark green color).

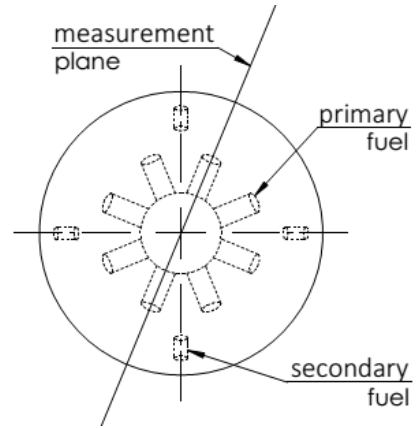


Fig. 3 — Top view of the lance and the location of the measurement plane relative to the primary and secondary fuel ports.

Imaging was performed using Photron Fastcam SA1.1 camera positioned perpendicularly to the laser sheet and adjusted to capture the images of illuminated particles seeded into the flow. The camera field of view was 107 x 107 mm, giving a pixel resolution 0.1 mm per pixel. Even though the flow field behind the lance is inherently of unsteady nature, time-averaged velocity components were used to analyze the flow field. The frequency of the laser and the camera was 1 kHz and for each test, 2000 image-pairs were acquired. Detailed information on PIV setup and PIV data processing procedure are given in Dutka et al. [37] and are not repeated here for brevity.

### 3. Results and discussion

#### 3.1. NO<sub>x</sub> emissions performance

##### 3.1.1. Effect of fuel power load and fuel mixture composition

Fig. 4 presents NO<sub>x</sub> emissions at various PPBB burner operating conditions as specified in Table 1. For burner thermal loads ranging from 10 to 25 kW, the characteristic temperature of the chamber wall measured to be 1050 - 1350°C using unshielded thermocouples. The lowest NO<sub>x</sub> emissions were achieved at a 10 kW power load with 55 mg/kWh ( $\equiv$  26 ppm @ 3% O<sub>2</sub> dry) and 102 mg/kWh ( $\equiv$  66 ppm @ 3% O<sub>2</sub> dry) for CH<sub>4</sub> and H<sub>2</sub> respectively. Both cases were

with the shorter lance position and therefore highest momentum flow, but with different fuel distribution. An increase in flow momentum, leading to an increase in turbulence and local stretch, has a positive consequence on the formation of  $\text{NO}_x$  [38] for thermal  $\text{NO}_x$ , but also to a lesser extent prompt  $\text{NO}_x$ . However, in a practical burner many direct and indirect effects prevent from drawing a general trend on  $\text{NO}_x$  by simple turbulence scaling. By increasing power load mass flow there are coupled effects of time scales at Kolmogorov scales, radical formation and non-equilibrium effects [39] and other indirect parameters, such as variation in radiative heat loss by soot formation or higher degree of local mixing [38]. Furthermore increase of  $\text{NO}_x$  emissions with thermal load is generally encountered in combustion devices [40] and justified as a consequence of a general increase in temperature due to higher power density and lower heat losses. The effect of increasing the  $\text{H}_2$  content in the fuel on  $\text{NO}_x$  is widely reported and the ratio between pure  $\text{CH}_4$  and  $\text{H}_2$  flames on the same burner can be as high as 3 depending on the burner configuration [4,21-25]. In the PPBB burner case, this ratio is about two, and the  $\text{CH}_4/\text{H}_2$  (50/50) case lies in between. The effect of  $\text{H}_2$  is a combined consequence of increased temperature promoting thermal NO and formation of radicals (O, H, OH) affecting prompt NO. The macro combustion properties of  $\text{H}_2$  as fuel in terms of increased flame speed, preferential diffusion, and reduced auto-ignition delay time all play negatively for all burner designs attempting to achieve a certain degree of premixing in recirculation stabilized flames such as swirl or bluff body.

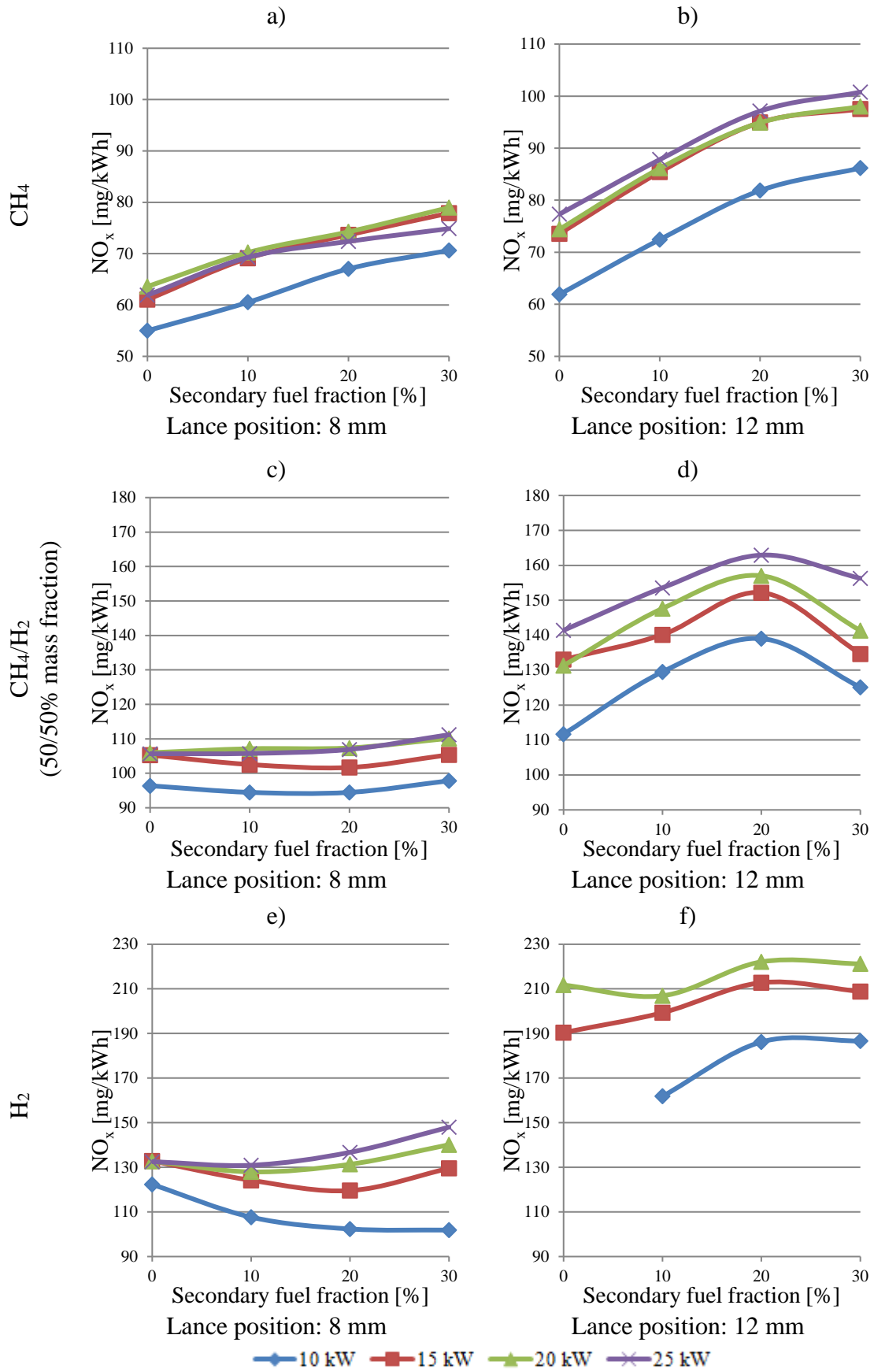


Fig. 4 — NO<sub>x</sub> emission performance of the PPBB burner as a function of thermal load, different configurations and fuels.

### 3.1.2. Effect of burner lance position

Low  $\text{NO}_x$  burners are able to achieve  $\text{NO}_x$  emissions lower than equilibrium concentrations because they play on aerodynamic features to mitigate its formation in the flame. In the PPBB burner, these features can be optimized by adjusting lance position and secondary fuel distribution. For all the tested fuels, shifting the lance downstream of the burner throat implies increased  $\text{NO}_x$  emissions, as shown for two selected positions in Fig. 4. This is in good agreement with the results of previous measurements conducted by Dutka et al. [35,36] and confirms the trend observed therein for lance positions 13–25 mm. The position of the lance in the burner affects directly the velocity of the air flow and in turn, the strain rates, residence times and turbulent flow field in the burner. The effect of inlet velocity on  $\text{NO}_x$  emissions in bluff body stabilized flames was already observed by Dally et al. [29] to decrease the amount of  $\text{NO}_x$  produced in the recirculation zone through a shortening of the residence time. However, their bluff body burner was of non-premixed type with obviously stronger mixture fraction stratification. As it was seen in our previous study [37] and in the next sections describing the turbulent flow, that the recirculation zone size decreases with an increase in air velocity resulting from a shorter lance position. In the case of the PPBB burner, the lance position is also affecting the quality of fuel-air mixing.

At higher lance positions, primary fuel ports are located at the narrower sections of the outer tube, where the combustion air reaches higher velocities. This leads to a lesser penetration of the fuel jets and therefore mixing. For the  $\text{CH}_4$  case at a thermal load of 10 kW, the jet penetration length calculated by the single jet penetration correlation from Lefebvre [41] and assuming flat velocity profiles is 4.9 mm and decreasing to 2.9 mm, when the lance position is moved from 8 mm to 12 mm respectively. Furthermore, high velocities at the burner throat may result in an increased entrainment of the combustion chamber flue gas by the air stream that acts as internal flue gas recirculation, decreasing the temperature in the combustion zone. From Fig. 4, shifting the lance from 8 to 12 mm increases  $\text{NO}_x$  emissions from 55 mg/kWh to 62

mg/kWh in the case of CH<sub>4</sub> and from 102 mg/kWh to 162 mg/kWh in the case of H<sub>2</sub>. High NO<sub>x</sub> emissions above 187 mg/kWh for H<sub>2</sub> at a lance position 12 mm may be partly caused by the fact that the H<sub>2</sub>/CH<sub>4</sub> flames and the H<sub>2</sub> flames were stabilized below the top surface of the bluff body as a result of lower velocity and high H<sub>2</sub>-air flame speed. It would result in combustion taking place near the fuel ports and probably inside the outer tube in non-premixed mode. Examination of the lance after these tests revealed that it was scorched at a certain distance below the top surface of the bluff body and therefore an evidence that the burner did not operate in desired conditions. A general behavior observed for CH<sub>4</sub> containing flames illustrated in Fig. 5 is that shifting the lance closer to the burner throat, is accompanied by an increase in CO emissions and lower flame stability.

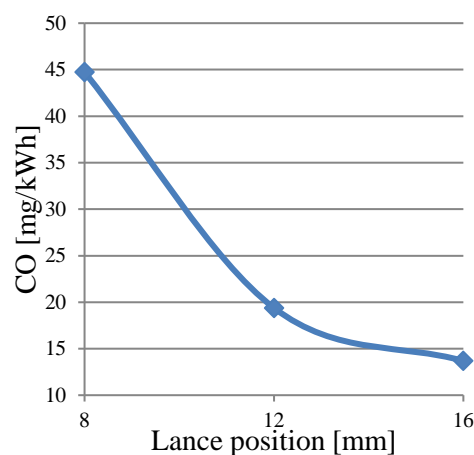


Fig. 5 — Effect of lance position on CO emissions at thermal load 25 kW and CH<sub>4</sub> as fuel.

### 3.1.3. Effect of secondary fuel distribution

The influence of secondary fuel stream on NO<sub>x</sub> emissions depends on fuel composition, burner thermal load and lance position. Momentum of fuel jets and position of secondary fuel ports relative to burner throat change the effect of secondary fuel stream through the mixing pattern. This interaction of secondary fuel stream with other burner operation parameters is clearly visible in Fig. 4 a), c), and e). If only CH<sub>4</sub> is supplied to the burner, NO<sub>x</sub> emissions tend to increase with increasing secondary fuel fraction (Fig. 4 a), b)). This negative effect is similar to

the findings of Dutka et al. [36] for secondary fuel fractions up to 20 %, and was also observed with CH<sub>4</sub>/H<sub>2</sub> mixtures containing up to 30 % of H<sub>2</sub> by mass and lance positions 13-20 mm. A different trend is seen for CH<sub>4</sub>/H<sub>2</sub> (50/50) as fuel, where the secondary fuel stream does not significantly change NO<sub>x</sub> emissions at a lance position of 8 mm, and peaking at around 20 % of secondary fuel fraction when the lance is located at 12 mm from the burner throat (see Fig. 4 c and d). Furthermore, there is an indication that a secondary fuel stream can be used to minimize NO<sub>x</sub> emissions when pure H<sub>2</sub> is used as fuel. For H<sub>2</sub> fuel only, according to Fig. 4 e), the burner generates minimum amount of NO<sub>x</sub> at the lowest thermal load tested, i.e., 10 kW, and at 30 % secondary fuel fraction. With increasing thermal load up to 20 kW, secondary fuel fraction should be decreased to 10% to ensure minimum NO<sub>x</sub> emissions. At thermal load equal to 25 kW, increasing secondary fuel fraction has a negative impact on NO<sub>x</sub> emissions as for the CH<sub>4</sub> fuel cases. Looking at the general trend of increasing the amount of secondary fuel split on NO<sub>x</sub> emissions shows that secondary fuel distribution can be seen as a way to minimize NO<sub>x</sub> emissions when shifting from one fuel to another.

In the investigated CH<sub>4</sub> and H<sub>2</sub> cases, if the lance is shifted downstream to 12 mm, NO<sub>x</sub> emissions do not decrease with increasing secondary fuel. It is believed that the secondary fuel has a stabilizing effect on the flame, as at lance position of 12 mm and a thermal load 10 kW, the flame extinguishes if all the fuel is supplied only through primary fuel ports, but combustion is sustained when portion of the fuel is supplied through secondary fuel ports. Nevertheless, at a lance position 12 mm the flame is stabilized below the top surface of the lance when H<sub>2</sub> is combusted and it always results in high NO<sub>x</sub> emissions without any particular trend for various thermal loads, as the flame regime is not controlled anymore by the bluff body flow. Worth noting, is that the variations in NO<sub>x</sub> observed and commented herein are always accompanied with CO levels, which indicate that the operation conditions are within acceptable combustion efficiency.

NO<sub>x</sub> emissions follow the same trends for various thermal loads tested in case of CH<sub>4</sub> used as fuel, as shown in Fig. 4 a), c), and e). Dutka et al. [37] has found that for the investigated burner geometry, the flow self-similarity regime in non-reacting conditions starts at Re = 19600. The burner certainly operates in this regime and for higher thermal loads, NO<sub>x</sub> emissions follow the same trends as for lower thermal loads. Another factor affecting mixing at molecular levels with H<sub>2</sub> as fuel constituent is its high diffusivity, what in turn may result in changes of NO<sub>x</sub> emissions [42].

### **3.2. Influence of wall temperature on NO<sub>x</sub> emissions**

Despite the fact that NO<sub>x</sub> are formed inside the flame, their production is affected by the surrounding environment and the combustion chamber conditions. It was observed that while all other operating parameters being the same, NO<sub>x</sub> emissions increase with increasing chamber temperature. This well-documented finding results from decreased radiative heat losses from the flame, which in turn increases local flame temperature and is essential to quantitatively predict NO<sub>x</sub> emissions [20,43].

With more and more stringent emissions limits, it is therefore important to study and quantify the NO<sub>x</sub> performance of a burner with respect to the chamber dependent heat transfer conditions. NO<sub>x</sub> emissions measured for CH<sub>4</sub> and H<sub>2</sub> combustion in the 700 – 1050 °C range of chamber wall temperatures are shown in Fig. 8. In this experiment, the burner was firing at settings corresponding to the cases CH4LP8SF0 and H2LP8SF30 defined in Table 2. Since the longitudinal temperature profile along of the chamber wall was not uniform, the highest measured temperature is used in Fig. 6.

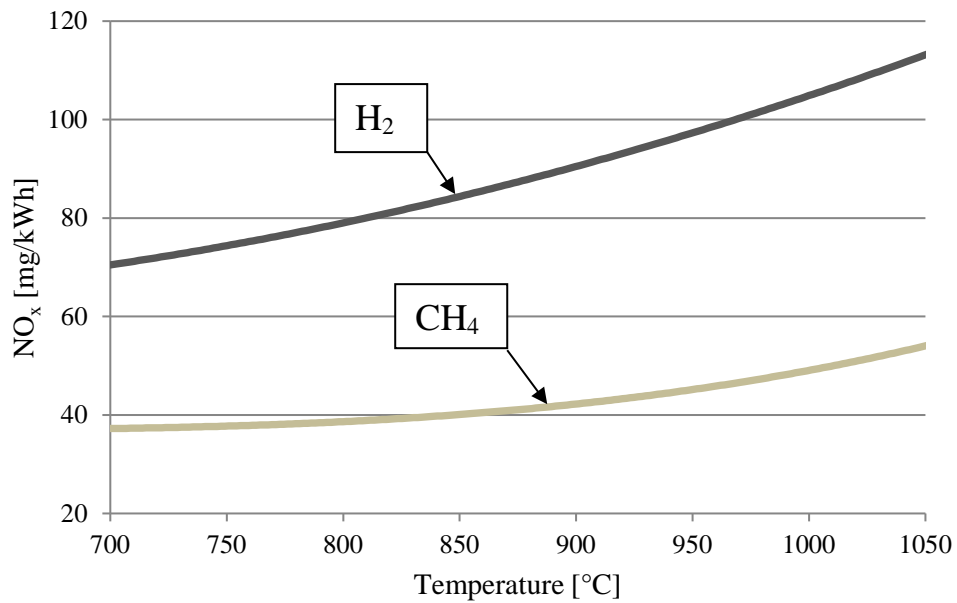


Fig. 6 — Effect of wall temperature on NO<sub>x</sub> emissions for different fuels.

The American Petroleum Institute (API) standard 535 provides a relationship describing the NO<sub>x</sub> emissions behavior of a burner as a function of furnace temperature [44,45]. This relationship is presented in Fig. 7 along with relative NO<sub>x</sub> emissions from CH<sub>4</sub> and H<sub>2</sub> combustion in the PPBB burner. The API standard overestimates NO<sub>x</sub> emissions compared with our data for both fuels, most likely due to the facts that it excludes any dependency to the burner used, nor does it account for the operating conditions such as excess air or fuel used [44]. The API 535 curve is based on firebox temperature measured in an industrial furnace, while in our case the highest measured chamber temperature was used. This may also cause certain deviations from the API 535 curve. Nevertheless, Fig. 7 shows that the PPBB burner is less sensitive to the firebox temperature than commonly used industrial burners.

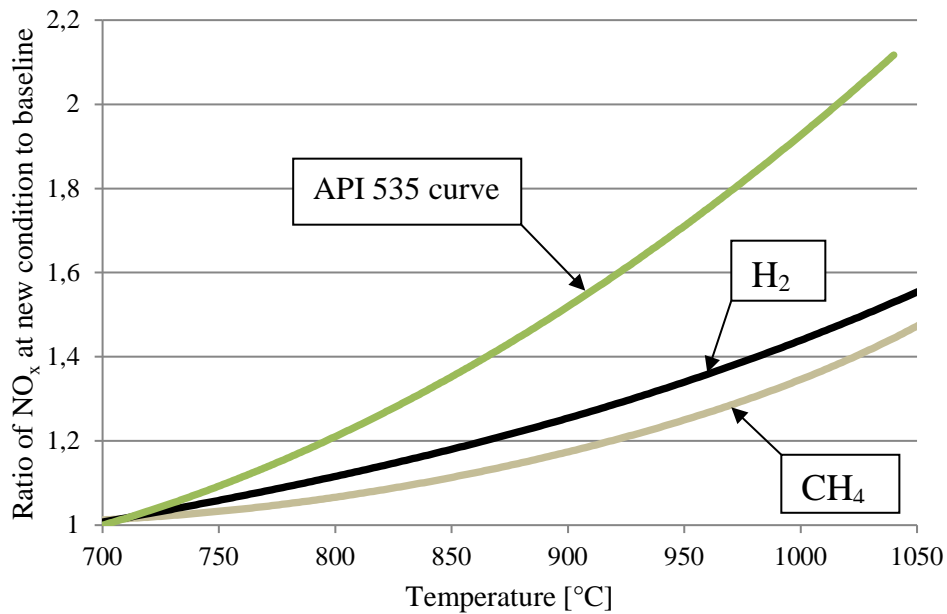


Fig. 7 — Sensitivity of NO<sub>x</sub> performance to firebox temperature.

From Figs. 6 and 7 it can be seen that the PPBB temperature dependency characteristics are also fuel dependent. In the temperature range 700 – 1050 °C, when the burner is fueled by CH<sub>4</sub>, NO<sub>x</sub> emissions increase from 36 mg/kWh to 54 mg/kWh. With H<sub>2</sub>, the increase in emissions is from 72 mg/kWh to 112 mg/kWh. These values correspond to a 1.5 and 1.55 fold increase for CH<sub>4</sub> and H<sub>2</sub>, respectively, higher than the 2.2 increase predicted from the API 535 standard. In addition, curves for CH<sub>4</sub> and H<sub>2</sub> shown in Fig. 7 show that NO<sub>x</sub> emissions from H<sub>2</sub>-air flames are slightly more sensitive to temperature of the chamber compared to those from CH<sub>4</sub>-air flames. Temperature distribution in the chamber might have changed for CH<sub>4</sub> and H<sub>2</sub> cases. The variation in heat flux in the chamber can have an impact on the different characteristics of CH<sub>4</sub> and H<sub>2</sub> flames presented in Figs. 6 and 7. However, it is believed not to be significant, because differences between the three measured temperature points along the wall were relatively constant across the investigated temperature range. The most probable explanation of the higher sensitivity of H<sub>2</sub>-air flame is a combined effect of a higher temperature in conjunction with the exponential dependency on temperature of the thermal NO<sub>x</sub> formation mechanism. Consequently, the same flame temperature gain induced by lower radiation loss results in a

stronger increase in  $\text{NO}_x$  with the  $\text{H}_2$  flames. Furthermore, thermal  $\text{NO}_x$  formation mechanism contributes more to total  $\text{NO}_x$  formation in  $\text{H}_2$ -air flames than in  $\text{CH}_4$ -air flames, where the less temperature sensitive prompt route should also be taken into account.

### **3.3. Turbulent flow field**

The effect of the flow field structure and turbulence on the  $\text{NO}_x$  chemistry is a classical and critical topic. In order to better understand this interaction in the PPBB burner the near-field aerodynamics has been investigated by PIV for selected configurations (cf. Table 2). The intention is to examine the flow field at the most promising burner operation settings with  $\text{CH}_4$  and  $\text{H}_2$  as fuel. In addition, since the secondary fuel fraction has different impact on  $\text{NO}_x$  emissions depending on whether the burner operates with  $\text{CH}_4$  or  $\text{H}_2$ , PIV was applied to cases with 0 % and 30 % secondary fuel fraction. As noted in the experimental description section, PIV measurements were made without confinement as the area of interest is the near field. It is however such that when the burner is fueled with  $\text{CH}_4$  at 8 mm lance position the flame is stable and performing well (see Fig. 4), but without the chamber the flame becomes very unstable. Therefore, only non-reacting cases were investigated at this position with  $\text{CH}_4$ . To study the effect of the lance position on non-reacting flow PIV measurements with  $\text{CH}_4$  at lance position of 16 mm was made, both reacting and non-reacting (cf. Table 2).

#### **3.3.1. Description of the flow field**

Velocity flow fields for the selected cases from Table 2 are shown in Fig. 8. The general flow field structure is composed of an annular flow with axial momentum surrounding a recirculation zone characterized by three average stagnation points. One positioned at the burner centerline delimitating the recirculation zone and the downstream axial jet flow. It is also sometimes referred to as the neck [32]. The two other points in the 2D representation shown in Fig. 8 is in fact the center of an average 3D toroidal vortex structure. As seen from the velocity vectors, this is the structure feeding fresh reactants into the recirculation, as well as bringing hot products

of combustion at the shear layer. The latter has the effect of igniting the annular flow thus forming two distinct combustion regimes, merging after the neck. In the non-reacting cases, combustion do not bring additional momentum through volume expansion and the near field has much lower velocity levels. Note that the instantaneous flow fields corresponding to the cases shown in Fig. 8 diverge greatly from this average structure picture. Examples can be found in Dutka et al. [37] and indicate that the toroidal structure is strongly asymmetric and probably breaks up in an intermittent manner, adding to the turbulence levels as will be shown in the following section. This overall structure is the same for all cases and the parameters varied in this study only affect the intensity, size and position of the different features. The PPBB burner configuration differs from more traditional bluff body burners where the fuel is injected through a central nozzle. A central jet has the effect of generating an additional inner vortex zone [29,32-34], not present in the PPBB, and the local equivalence ratio is much more stratified as the configuration is non-premixed.

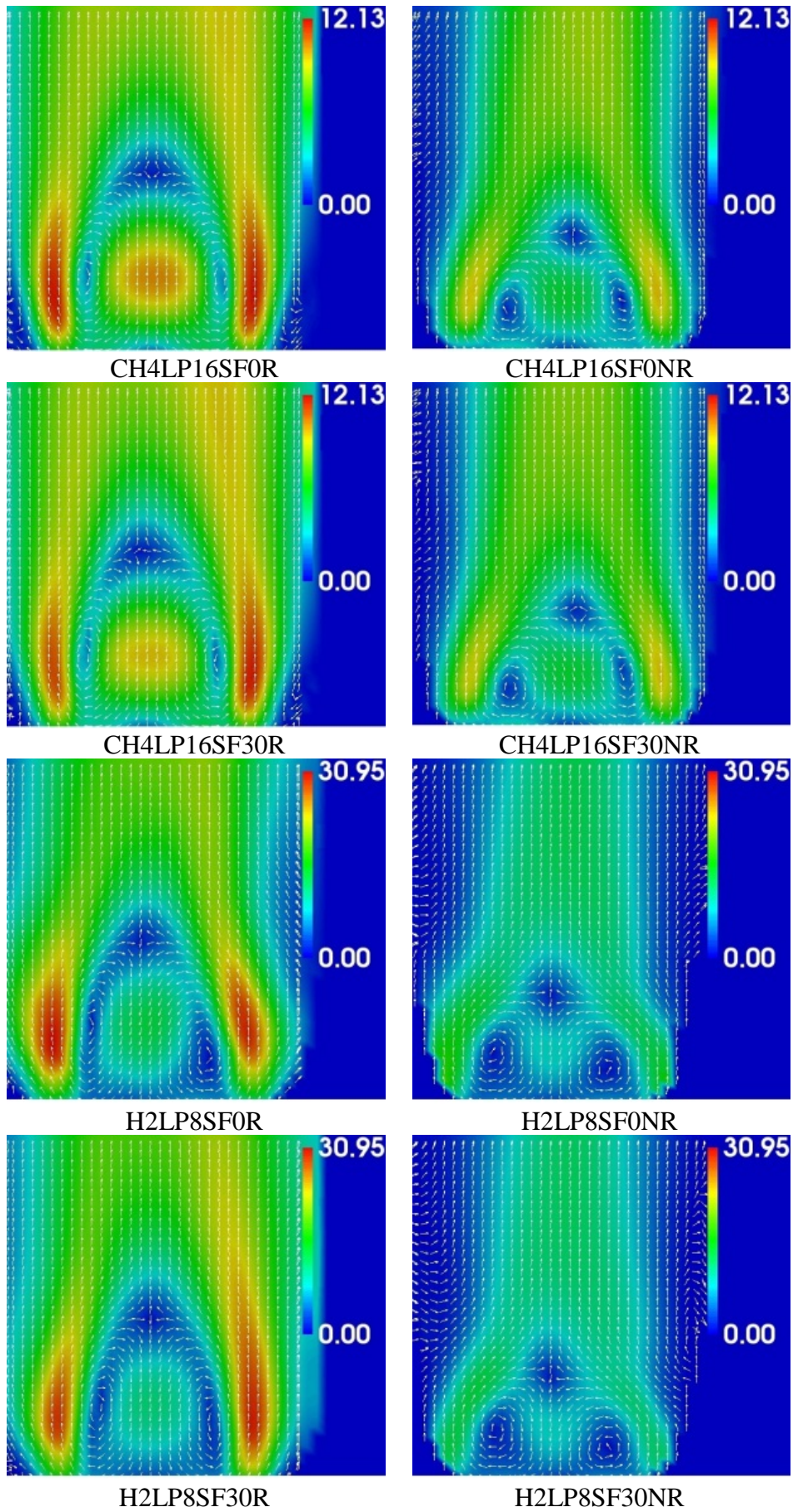


Fig. 8 — Velocity contour plots and vectors for the investigated cases. Color intensity represents velocity in m/s.

### 3.3.2. Effect of burner lance position

By shifting the lance from 8 to 16 mm the throat air velocity is decreased by almost 2.9 times. Despite this significant difference, the velocities in the post recirculation zone are only approximately 1.6 times lower, because the flow goes through a sudden expansion and decelerates considerably before the trailing edge of the lance. Fig. 9 shows axial velocity profiles at lance positions 8 and 16 mm along the centerline, where the length of the recirculation zone is determined when the axial velocity crosses zero. The profiles reveal that the length of the recirculation zone is increased from 17.7 mm to 19.7 mm when the lance is shifted from 8 mm to 16 mm. Although minor, this increase is clearly discernable given the PIV setup resolution [37].

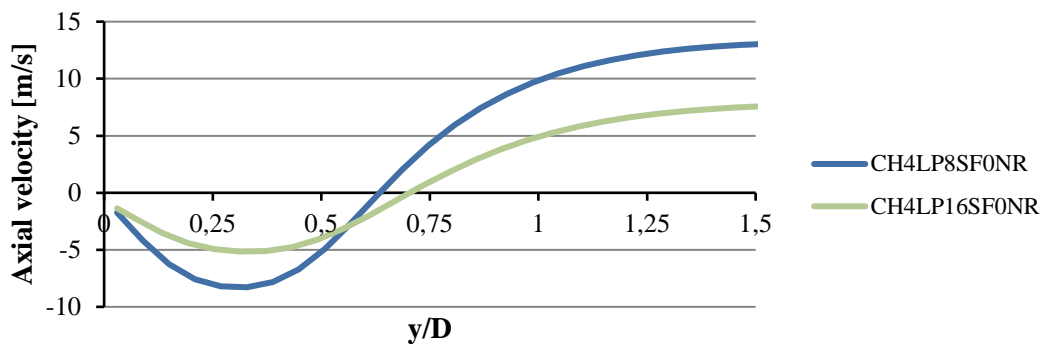


Fig. 9 — Axial velocity along the centerline of the PPBB burner for two lance positions: 8 and 16 mm.

The corresponding cases with combustion are shown in Fig. 10. The flames are stabilized behind the lance at the shear layer, between the main stream and the recirculation zone. When the lance is shifted downstream from 8 mm to 16 mm, the curvature of the flame decreases, indicating that the length of the recirculation zone expands in the axial direction as shown in the axial velocity profiles in the non-reacting cases.

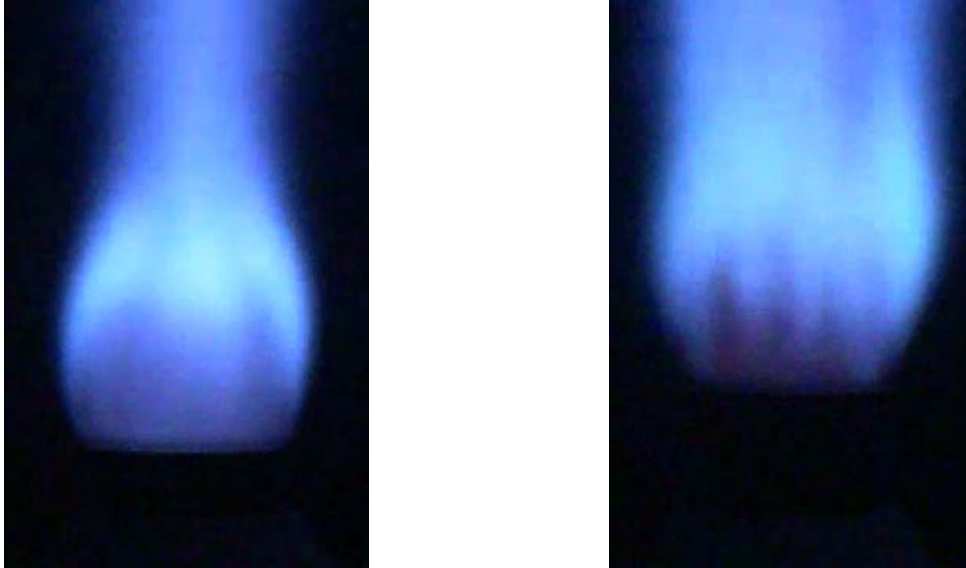


Fig. 10 — Photos of CH<sub>4</sub>-air flame stabilized behind the lance of the PPBB burner for two lance positions: 8 mm (LHS) and 16 mm (RHS).

Shifting the lance changes simultaneously two factors that affect the flow field: the throat velocity and the geometry of the burner. Indeed, the flow path from the burner throat to the bluff body increases with increasing lance position, leading to a greater velocity decay of the flow before it reached the bluff body front. This affects the recirculation process that is dependent on the velocity at the edge of the bluff body. In order to dissociate the two parameters, Fig. 11 shows the axial velocity profiles obtained at an 8 mm lance position, with one case being design conditions and the other obtained by decreasing the air mass flow rate such as to match the burner throat velocity matching that of a 12 mm lance position. The influence of the throat velocity on the length of the recirculation zone can then be analyzed, as this reduction in air mass flow rate led to a reduction of burner throat velocity from 36.8 to 18.9 m/s in the CH<sub>4</sub> case, and from 38.1 to 19.6 m/s in the H<sub>2</sub> case. Even though the velocity is reduced by almost half, the length of the recirculation zone is barely affected (less than a millimeter and 1 mm for CH<sub>4</sub> and H<sub>2</sub> respectively). It is in good agreement with the previous work by Dutka et al. [37] in non-reacting flows where it was found that in the turbulent regime the length of the recirculation zone does not depend significantly on the inlet velocity.

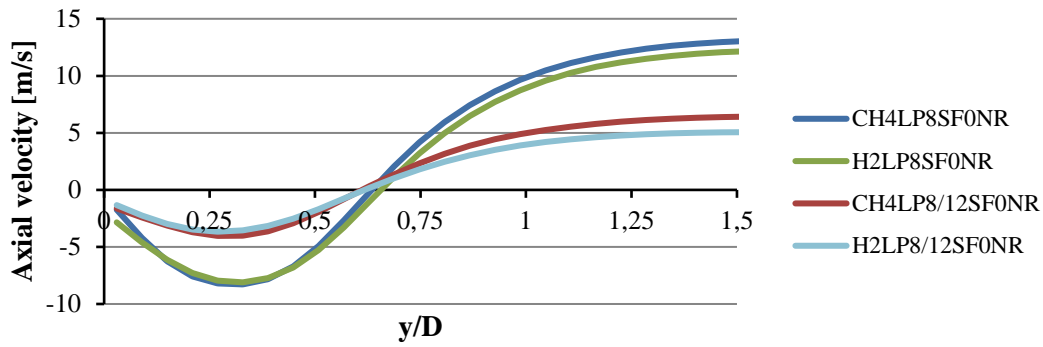


Fig. 11 — Axial velocity along the centerline of the PPBB burner for lance position fixed at 8 mm and nominal and reduced air mass flow rates.

These results indicate that in the turbulent regime the effect of the lance position on the length of the recirculation zone is caused by the burner geometry rather than the burner throat velocity. Even if significant decrease in velocity results in shortening of the recirculation zone (cf. Fig. 11), while shifting the lance downstream increases the length of the recirculation zone (cf. Fig. 9).

### 3.3.3. Effect of secondary fuel fraction

From the PIV data presented in Fig. 8 the secondary fuel fraction does not seem to affect the flow field above the bluff body. It is important to note that the measurement plane did not cross the secondary fuel ports (cf. Fig. 4), hence the effect of secondary fuel is not fully captured. It can be assumed that the secondary fuel stream may affect the velocity of the air-fuel mixture locally, but not to such an extent as to modify the global recirculation zone behavior. This is further confirmed in the velocity profiles of Fig. 12 in non-reacting flows with both H<sub>2</sub> and CH<sub>4</sub>. In the cases with combustion however, the fuel distribution strategy affects the flow field through a different fuel and local equivalence ratio distribution. These changes are seen to be limited to the recirculation zone only. It can be also seen in Fig. 8 and 12 that the region of high velocity in the recirculation zone is slightly reduced when fuel is partly injected through the secondary fuel ports. This can be explained by the fact that secondary fuel being injected in

cross-flow relative to the air stream locally decelerates the axial component of the flow, resulting in slightly lower velocities in the recirculation zone.

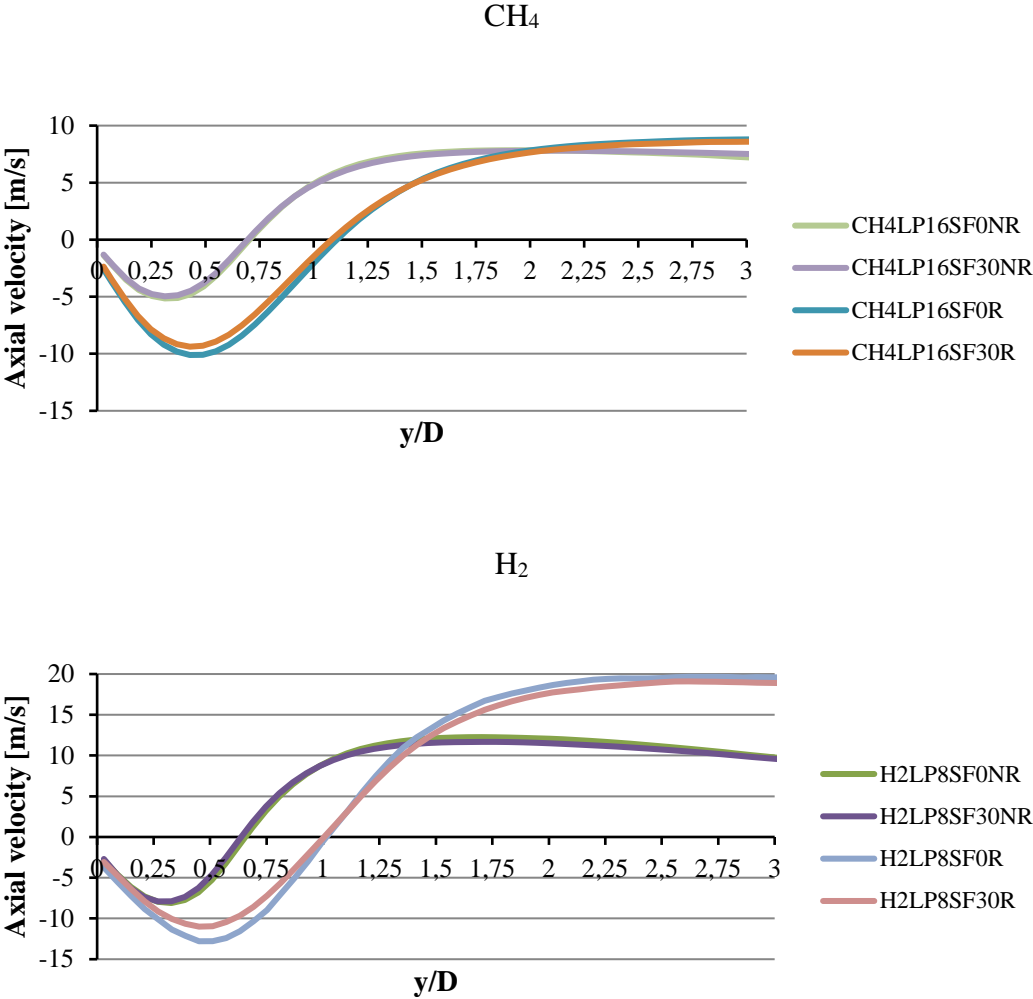


Fig. 12 — Axial velocity along the centerline of the PPBB burner.

**3.3.4. Near field turbulence**

The presence of the flame causes the volume of the recirculating gas to increase. From Fig. 12 it is observed that combustion affects the length of the recirculation zone changing from 19.7 mm (non-reacting) to 31 mm (reacting) for CH<sub>4</sub> and from 18.3 mm to 28.5 mm for H<sub>2</sub>. For both

CH<sub>4</sub> and H<sub>2</sub> it increases 1.5 times when the flame is present and seems to be independent of the lance position. Quantitatively, however, the length of the recirculation zone is greater for CH<sub>4</sub> than for H<sub>2</sub>. It can be the effect of the lance position, because the elongation of the recirculation zone when the lance is shifted downstream of the burner throat was observed in non-reacting flows.

Velocities measured in Fig. 12 are larger in reacting flows because of volumetric expansion caused by combustion. The difference that can also be seen visually in Fig. 8 is much higher with H<sub>2</sub> than with CH<sub>4</sub> due to the obvious higher flame temperatures and the larger volume required for an equal input fuel power. For H<sub>2</sub> the maximum velocity downstream of the lance is nearly 20 m/s in reacting case and 11.6 m/s in non-reacting case. Such difference is not observed for CH<sub>4</sub> where the maximum velocity is 8.6 m/s for reacting flow and 7.2 m/s for the non-reacting flow.

Turbulent kinetic energy ( $= 0.5(u'^2 + 2*v'^2)$ ) of the flow field changes significantly between non-reacting and reacting flows as shown in Fig. 13. A notable phenomenon observed is the large production of turbulent energy inside the recirculation zone. The stagnation points at the center of the vortices have shown to have large-scale intermittent motion [37] that adds to the turbulence kinetic energy without necessarily participating to small scale mixing controlling combustion as discussed in Schefer et al. [33]. The high levels of turbulence does however participate in straining the flame front and interact with the NO<sub>x</sub> chemistry.

The disparity between non-reacting and reacting cases is caused by large density difference between the incoming fresh mixture and products in the recirculation zone as well as from the fluctuating pressure field due to volumetric expansion during combustion [46]. In all cases the strongest zone of turbulence is at the base of the shear layer between streamlines keeping an axial momentum and those which are drawn into the recirculation zone.

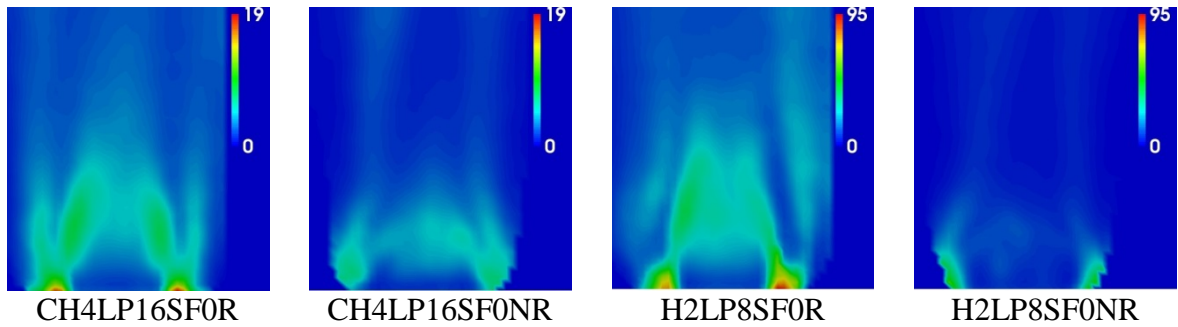


Fig. 13 — Turbulent kinetic energy intensity ( $\text{m}^2/\text{s}^2$ ) in non-reacting and reacting cases with  $\text{CH}_4$  and  $\text{H}_2$  as fuels.

### 3.4 Discussion

$\text{NO}_x$  formation depends on temperature, chemical kinetics largely affected by fuel composition and air-fuel equivalence ratio. Because turbulent mixing affects the local temperature and stoichiometry, any parameters influencing the flow field can affect  $\text{NO}_x$  formation. One such parameter in the PPBB burner is the lance position that directly affects the burner throat velocity. Measurements of  $\text{NO}_x$  emissions presented in Fig. 4 revealed that  $\text{NO}_x$  can be reduced when the lance is shifted such as to reduce the cross sectional area, resulting in an increase of velocities at the base of the bluff body, in the recirculation zone and in the jet like part of the flame as shown in Fig. 11. Fuel is always provided to the burner inside the air annular duct, where the air-fuel mixture is accelerated. It then undergoes a sudden expansion at the burner throat before being ignited behind the bluff body. Higher velocities, deeper penetration of the fuel jets in the air, and increased turbulence at the burner throat (cf. Fig. 13) imply enhanced mixing of fuel and air before it enters flame stabilization zone. In addition, higher velocities enhance the volume of entrained flue gases from the combustion chamber that mixes with the fresh reactants prior to the combustion zone.

In sufficiently fuel lean premixed conditions, low  $\text{NO}_x$  can be achieved. Additionally beneficial for controlling  $\text{NO}_x$  formation is to realize a degree of flue gas recirculation either internal or external. Achieving good mixing of fuel and air for operating in premixed combustion mode is therefore of utmost importance for low  $\text{NO}_x$  burners similar to the PPBB burner. The burner

tested in fuel lean conditions and uniform fuel distribution around the lance due to high velocities of air-fuel mixtures makes the flame similar to premixed flames. However, when the velocity at the burner throat is decreased by shifting the lance downstream, the generation of turbulent kinetic energy is reduced and therefore fuel and air mixing quality decreases, as shown in Fig 14. This configuration makes the flame more diffusion-like than premixed as seen in Fig. 11, where single separate flames emanating from the fuel nozzles can be evidenced, resulting in increased  $\text{NO}_x$  emissions.

Low  $\text{NO}_x$  can be usually achieved at conditions when flames are close to blow-off as noticed by Dally et al. [29].  $\text{NO}_x$  formation time-scale is long compared with other reactions in the flame and therefore  $\text{NO}_x$  does not reach maximum equilibrium value when the flame is close to blow-off at a given temperature. It was found that shifting the lance downstream improves flame stability, decreases CO emissions, and lowers the tendency to blow-off events, but at the expense of increased  $\text{NO}_x$  emissions. The better flame stability is caused by lower inlet throat velocity which is one of the main parameters controlling the stability limits of a flame [47].

From Fig. 4 it is seen that secondary fuel stream causes an increase of  $\text{NO}_x$  emissions and it is generally better to provide fuel to the burner through the primary fuel ports. The only exceptions are  $\text{H}_2$ -air flames at 10, 15 and 20 kW and lance position 8 mm, when increasing secondary fuel fraction leads to lower  $\text{NO}_x$  emissions. Based on the PIV results it is challenging to find the reason for this effect as they only revealed decreased velocities in the recirculation zone (Fig. 8 and 13). One reason could be that more fuel is transported from the annular flame to the region of higher strain rates in the recirculation zone. Other quantities such as fuel concentration or temperature fields would bring useful information for explaining the reduction of  $\text{NO}_x$  emissions in this particular case.

The positive effect of the secondary fuel stream is that it improves flame stability in some cases, as in the 10 kW  $\text{H}_2$ -air flame with a 12 mm lance position, which would otherwise extinguish.

Nevertheless,  $\text{NO}_x$  emissions from the  $\text{H}_2$  flames were very high at lance position 12 mm and it is unclear if these flames are actually stabilized above the bluff body or already near the fuel ports. If so, the burner operates in a mode closer to diffusion flame, therefore in conditions other than those it was designed for, which could explain the lack of a clear trend in  $\text{NO}_x$  emissions relative to secondary fuel fractions for the various thermal loads tested.

#### **4. Conclusions**

This study examined  $\text{NO}_x$  emissions from  $\text{CH}_4$  and  $\text{H}_2$  combustion and the velocity flow field in the PPBB burner. Measurements of  $\text{NO}_x$  emissions were conducted for burner thermal loads within the range of 10 - 25 kW and combustion chamber temperatures in the region 1050 - 1350 °C. PIV measurements were conducted to investigate how the flow field was affected by factors such as fuel type and burner design parameters. The main conclusions of the study are the following:

- 1) Lance position relative to the burner throat is an important design parameter that affects  $\text{NO}_x$  emissions and flame stability.  $\text{NO}_x$  emissions can be reduced by shifting the lance towards the burner throat, hence by increasing velocity of the inlet throat air-fuel mixture. This effect can be due to changes of the turbulent flow field behind the lance, changes in fuel-air mixing, as well as the entrainment of the combustion chamber flue gas into the combustion zone by the high velocity air stream. Shifting the lance towards the burner throat increases velocities and reduces the length of the recirculation zone behind the lance. This reduction of the length of the recirculation zone is not due to higher inlet throat velocity, but it is solely due to the modification of the burner geometry.
- 2) Secondary fuel provided to the burner always contributes to  $\text{NO}_x$  emissions increase with  $\text{CH}_4$ , but supplying 10 – 30 % of the fuel through secondary fuel ports can be beneficial for reducing  $\text{NO}_x$  emissions with  $\text{H}_2$  as fuel. However, this effect can be

achieved only if the burner operates at thermal loads between 10 - 20 kW and a lance position of 8 mm. Furthermore, PIV results revealed that secondary fuel fraction decreases velocities in the recirculation zone, but it does not have significant impact on the flow field further downstream.

- 3) Increasing the temperature of the chamber implies an increase in NO<sub>x</sub> emissions by approximately 1.5 times within a temperature range 700 - 1050 °C for both CH<sub>4</sub> and H<sub>2</sub>. Even moderate changes of firebox temperature at the high temperatures range may result in significant increase of NO<sub>x</sub> emissions.
- 4) The length of the recirculation zone above the bluff body increases by 50 % for reacting flow compared with non-reacting flow at identical flow conditions. This is caused by volumetric expansion of the flue gas produced in the flame. Velocities behind the lance increase in the case of reacting flow for the same reason and is intensified as H<sub>2</sub> is added to the fuel because of higher flame temperature and larger volume of reaction products.

## **Acknowledgments**

This publication has been produced with support from the BIGCCS Centre, performed under the Norwegian research program Centers for Environment-friendly Energy Research (FME). The authors acknowledge the following partners for their contributions: ConocoPhillips, Gassco, Shell, Statoil, TOTAL, GDF SUEZ and the Research Council of Norway (193816/S60).

## **References**

[1] IPCC, 2005: IPCC Special Report on Carbon Dioxide Capture and Storage. Prepared by Working Group III of the Intergovernmental Panel on Climate Change [Metz, B., O. Davidson, H. C. de Coninck, M. Loos, and L. A. Meyer (eds.)]. Cambridge University Press, Cambridge, United Kingdom and New York, NY, USA, pp. 77

- [2] Cormos C.C., Evaluation of power generation schemes based on hydrogen-fuelled combined cycle with carbon capture and storage (CCS), *Int J Hydrogen Energy*. 36:(2011) 3726-3738.
- [3] Schefer R.W., Hydrogen enrichment for improved lean flame stability, *Int J Hydrogen Energy*. 28 (2003) 1131-1141.
- [4] Cozzi F., Coghe A., Behavior of hydrogen-enriched non-premixed swirled natural gas flames, *Int J Hydrogen Energy*. 31 (2006) 669-677.
- [5] García-Armingol T., Ballester J., Operational issues in premixed combustion of hydrogen-enriched and syngas fuels, *Int J Hydrogen Energy*. 40 (2015) 1229-1243.
- [6] Emadi M., Karkow D., Salameh T., Gohil A., Ratner A., Flame structure changes resulting from hydrogen-enrichment and pressurization for low-swirl premixed methane-air flames, *Int J Hydrogen Energy*. 37 (2012) 10397-10404.
- [7] Frenillot J.P., Cabot G., Cazalens M., Renou B., Boukhalfa M.A., Impact of H<sub>2</sub> addition on flame stability and pollutant emissions for an atmospheric kerosene/air swirled flame of laboratory scaled gas turbine, *Int J Hydrogen Energy*. 34 (2009) 3930-3944.
- [8] Yon S., Sautet J.C., Boushaki T., Effects of burned gas recirculation on NO<sub>x</sub> emissions from natural gas-hydrogen-oxygen flames in a burner with separated jets, *Energy and Fuels*. 26 (2012) 4703-4711.
- [9] Ranga Dinesh K.K.J., Luo K.H., Kirkpatrick M.P., Malalasekera W., Burning syngas in a high swirl burner: Effects of fuel composition, *Int J Hydrogen Energy*. 38 (2013) 9028-9042.
- [10] Kim H.S., Arghode V.K., Gupta A.K., Flame characteristics of hydrogen-enriched methane-air premixed swirling flames, *Int J Hydrogen Energy*. 34 (2009) 1063-1073.
- [11] Rørtveit, G.J., Stromman, A.H., Ditaranto, M., Hustad, J.E., Emissions from combustion of H<sub>2</sub> and CH<sub>4</sub> mixtures in catalytic burners for small-scale heat and power applications, *Clean Air* 6(2005):187-191.
- [12] Ditaranto M., Li H., Hu Y., Evaluation of a Pre-combustion Capture Cycle Based on Hydrogen Fired Gas Turbine with Exhaust Gas Recirculation (EGR), *Energy Procedia* 63(2014):972-1975.
- [13] Ditaranto M., Li H., Løvås T., Concept of hydrogen fired gas turbine cycle with exhaust gas recirculation: Assessment of combustion and emissions performance, *International Journal of Greenhouse Gas Control* 37 (2015) 377–383.
- [14] Zeldovich Y.B., Sadovnikov P.Y., Frank-Kamenetski D.A., Oxidation of Nitrogen in Combustion, Academy of Sciences of USSR, Institute of Chemical Physics, Moscow-Leningrad 1947
- [15] Lavoie G.A., Heywood J.B., Keck J.C., Experimental and theoretical study of nitric oxide formation in internal combustion engines, *Combustion Sci. Technol.* 1 (1970) 313-326.

- [16] Fenimore C.P., Formation of nitric oxide in premixed hydrocarbon flames, *Symp. Int. Combust.* 13 (1971) 373-380.
- [17] Miller J.A., Bowman C.T., Mechanism and modeling of nitrogen chemistry in combustion, *Progress in Energy and Combustion Science.* 15 (1989) 287-338.
- [18] Konnov A.A., Colson G., De Ruyck J., NO formation rates for hydrogen combustion in stirred reactors, *Fuel.* 80 (2001) 49-65.
- [19] Rørtveit G.J., Hustad J.E, Li S., Williams F.A., Effects of diluents on NO<sub>x</sub> formation in hydrogen counterflow flames, *Combust. Flame.* 130 (2002) 48-61.
- [20] Turns S.R., Myhr F.H., Oxides of nitrogen emissions from turbulent jet flames: Part I-Fuel effects and flame radiation, *Combust. Flame.* 87 (1991) 319-335.
- [21] Wu, L.A , Kobayashi, N.A , Li, Z.B, Huang, H.C, Experimental study on the effects of hydrogen addition on the emission and heat transfer characteristics of laminar methane diffusion flames with oxygen-enriched air, *International Journal of Hydrogen Energy* 41(3) (2016):2023-2036.
- [22] El-Ghafour S.A.A., El-dein A.H.E., Aref A.A.R., Combustion characteristics of natural gas-hydrogen hybrid fuel turbulent diffusion flame, *International Journal of Hydrogen Energy* 35 (2010) 2556-2565.
- [23] Choudhary AR, Gollahalli SR. Combustion characteristics of hydrogen-hydrocarbon hybrid fuels. *Int J Hydrog Energy* 2000;25:451-2.
- [24] Choudhuri AR, Gollahalli SR. Characteristics of hydrogen-hydrocarbon composite fuel turbulent jet flames. *Int J Hydrog Energy* 2003;28:445-54
- [25] Ilbas, M, Yilmaz I. Experimental analysis of the effects of hydrogen addition on methane combustion. *Int J Energy Res* 2012;36:643-7.
- [26] Waibel R.T., Athens L.; Claxton M., Effect of fuel composition on emissions from ultra low NO<sub>x</sub> burners. In *Proceedings of the International Symposium Combustion Research and Industrial Practice: From Equations to Equipment*, Monterey, CA, USA, 15-18 October 1995.
- [27] Ayoub M, Rottier C, Carpentier S, Villermaux C, Boukhalfa AM, Honore D. An experimental study of mild flameless combustion of methane/hydrogen mixtures. *Int J Hydrog Energy* 2012;37:6912-21
- [28] Newbold G.J.R., Nathan G.J., Nobes D.S., Turns S.R., Measurement and prediction of NO<sub>x</sub> emissions from unconfined propane flames from turbulent-jet, bluff-body, swirl, and precessing jet burners, *Symp. Int. Combust.* 28 (2000) 481-487.
- [29] Dally B.B., Masri A.R., Barlow R.S., Fiechtner G.J., Fletcher D.F., Measurements of no in turbulent non-premixed flames stabilized on a bluff body, *Symp. Int. Combust.* 26 (1996) 2191-2197.
- [30] Spangelo Ø., Sønju O.K., Slungaard Y., Ditaranto M. (2014) Method for burning of gaseous fuel and burner.

<http://www.google.com/patents/EP1989482A4?cl=en> (accessed on 21 September 2015)

- [31] Ditaranto M., Anantharaman R., Weydahl T., Performance and NO<sub>x</sub> emissions of refinery fired heaters retrofitted to hydrogen combustion, *Energy Procedia* 37 (2013) 7214-7220.
- [32] Dally B.B., Masri A.R., Barlow R.S., Fiechtner G.J., Instantaneous and Mean Compositional Structure of Bluff-Body Stabilized Nonpremixed Flames, *Combustion and Flame* 114:119–148 (1998)
- [33] Schefer R. W., Namazian M., Kelly J., Velocity measurements in turbulent bluff-body stabilized flows, *AIAA Journal*, Vol. 32, No. 9 (1994), pp. 1844-1851
- [34] Chen Y-C., Chang C-C., Pan K-L., Yang J-T., Flame Lift-off and Stabilization Mechanisms of Nonpremixed Jet Flames on a Bluff-body Burner, *Combustion and Flame* 115(1998):51-65.
- [35] Dutka M., Ditaranto M., Løvås T., Application of a central composite design for the study of NO<sub>x</sub> emission performance of a low NO<sub>x</sub> burner, *Energies* 8 (2015) 3606-3627.
- [36] Dutka M., Ditaranto M., Løvås T., Emission characteristics of the novel low-NO<sub>x</sub> burner fueled by hydrogen-rich mixtures with methane, *Journal of Power Technologies*, 95 (2015) 105-111.
- [37] Dutka M., Ditaranto M., Løvås T., Investigations of air flow behavior past a conical bluff body using particle imaging velocimetry, *Exp in Fluids*. 56(2015):199.
- [38] Turns S.R., Understanding NO<sub>x</sub> formation in nonpremixed flames: experiments and modelling, *Prog. Energy Combust. Sci.* 21(1995):361-385.
- [39] Barlow R.S., Carter C.D., Relationships among nitric oxide, temperature, and mixture fraction in hydrogen jet flame, *Combustion and Flame* 104(1996): 288-299
- [40] Mishra D.P., Jejurkar S.Y., Characterization of confined hydrogen-air jet flame in a crossflow configuration using design of experiments, *Int J Hydrogen Energy* 38 (2013) 5165-5175.
- [41] Lefebvre A.H., *Gas Turbine Combustion*, 2nd Ed., Taylor and Francis, Philadelphia, PA, 1999.
- [42] Gabriel R., Navedo J.E., Chen R., Effects of fuel Lewis number on nitric oxide emission of diluted H<sub>2</sub> turbulent jet diffusion flames, *Combust. Flame*. 121 (2000) 525-534.
- [43] Driscoll, J.F., Chen, R.H., and Yoon, Y. "Nitric Oxide Levels of Turbulent Jet Diffusion Flames: Effects of Varying Residence Time and Damkohler Number", *Combust. Flame* 88:37-49, 1992.
- [44] American Petroleum Institute, *Burners for Fired Heaters in General Refinery Services*, API Recommended Practice 535, 2nd edn., American Petroleum Institute, Washington, DC, January 2006.

[45] Bussman W., Baukal C., Colannino J., The effect of firebox temperature on NOx emissions, Proceedings of the Air and Waste Management Association's Annual Conference and Exhibition, AWMA. (2004).

[46] Pope S.B., Turbulent premixed flames, Annual Review of Fluid Mechanics, 19 (1987) 237-270

[47] Frolov S.M., Basevich V.Y., Belyaev A.A., Mechanism of turbulent flame stabilization on a bluff body, Chemical Physics Reports. 18 (2000) 1495-1516.